# Dieses Dokument ist eine Zweitveröffentlichung (Verlagsversion) /

# This is a self-archiving document (published version):

Guojiang Wan, Bo Lv, Guoshou Jin, Manfred F. Maitz, Jianzhang Zhou, Nan Huang

**Direct correlation of electrochemical behaviors with anti-thrombogenicity of semiconducting titanium oxide films**

Diese Version ist verfügbar / This version is available on:

https://nbn-resolving.org/urn:nbn:de:bsz:14-qucosa2-356943

**SLUB**
Wir führen Wissen.

**TECHNISCHE UNIVERSITÄT DRESDEN**

**Qucosa**
Quality Content of Saxony

Article

# Direct correlation of electrochemical behaviors with anti-thrombogenicity of semiconducting titanium oxide films

Guojiang Wan[1], Bo Lv[1], Guoshou Jin[1], Manfred F Maitz[1,2], Jianzhang Zhou[3] and Nan Huang[1]

## Abstract
Biomaterials-associated thrombosis is dependent critically upon electrochemical response of fibrinogen on material surface. The relationship between the response and anti-thrombogenicity of biomaterials is not well-established. Titanium oxide appears to have good anti-thrombogenicity and little is known about its underlying essential chemistry. We correlate their anti-thrombogenicity directly to electrochemical behaviors in fibrinogen containing buffer solution. High degree of inherent n-type doping was noted to contribute the impedance preventing charge transfer from fibrinogen into film (namely its activation) and consequently reduced degree of anti-thrombogenicity. The impedance was the result of high donor carrier density as well as negative flat band potential.

## Introduction

Biomaterials-associated thrombosis is of topical concern in biocompatibility of materials, in particular for blood-contacting implantable biomaterials.[1–4] Almost all natural and synthetic materials explored so far tend to induce an extent of thrombogenicity on surface when in contact with blood. Basically, the foreign surface induces coagulation cascade reactions which usually start from the activation of coagulating factors. For instance, the first coagulating factor protein fibrinogen is absorbed on the surface initially and is activated, then triggers the cascade and finally terminates with formation of fibrous clots, during which accompanying interactions with platelets and other coagulating factors occur. The anti-thrombogenicity of biomaterials is dependent upon the nature of the solid surface and more critically upon the interfacial phenomena between biomaterials and blood, i.e. interactions of proteins and platelets with surfaces. Extensive efforts have been taken to study the thrombogenic behaviors of biomaterials and develop desired anti-thrombogenic materials.[5] Surface modification with blood compatible film/coating is noted as an important strategy. Among them, titanium oxide film

appears to be relatively anti-thrombogenic as compared to even low-temperature-isotropic-pyrolytic-carbon as the commonly used fabricating material for artificial heart valve.[6,7] Intensive investigations have been carried out to find its good anti-thrombogenicity mainly due to its unique semiconducting property.[7–14] Nevertheless, titanium oxide films out of same technique do not possess same degree of anti-thrombogenicity, even when they seem to have large extent of similarity in surface characteristics. Underlying chemistry of interactions between film and coagulating factors might be decisive in fathoming

[1]Key Laboratory of Advanced Technologies of Materials, Ministry of Education, College of Materials Science and Engineering, Southwest Jiaotong University, Chengdu, China
[2]Max Bergmann Center of Biomaterials Dresden, Leibniz Institute of Polymer Research Dresden, Dresden, Germany
[3]State Key Laboratory of Physical Chemistry of the Solid Surface, Xiamen University, Xiamen, China

**Corresponding author:**
Guojiang Wan, Key Laboratory of Advanced Technologies of Materials, Ministry of Education, College of Materials Science and Engineering, Southwest Jiaotong University, Chengdu 610031, China.
Email: guojiang.wan@home.swjtu.edu.cn; superwgj@263.net; guojiang.wan@googlemail.com

anti-thrombogenicity mechanism, screening and designing of blood compatible biomaterials.

Activation of fibrinogen on surface is crucial in the coagulation process.[3] One hyposthesis suggests that such activation is characterised with an electrochemical interfacial charge tranfer reaction from fibronogen into solid surface.[15–17] The ease of electrochemical charge transfer seems to be the most important determinant of thrombogenicity on biomaterials, which is determined mainly by the electrochemical behavior of the materials with fibrinogen in blood. Preventing charge transfer is particularly effective and has been illustrated for semi-conducting titanium oxide and silicon carbide.[6,18] Nevertheless, there is rarely experimental correlation between the electrochemical behaviors of such semi-conducting biomaterials and their anti-thrombogenicity.[19–21]

The aim of this work is to ascertain the essential relationship between electrochemical response of titanium oxide to fibrinogen and its anti-thrombogenic performance. Titanium oxide films with different stoichiometry were obtained with vacuum deposition process to have different semiconducting properties. The prepared titanium oxide films were compared and analyzed in electrochemical behaviors in fibrinogen containing phosphate buffer solution as well as their anti-thrombogenic evaluations of fibrinogen denaturalization, platelets adhesion and clotting time. Electronic structure and energetics of titanium oxide films in contact with blood account for the extent of impedance of charge transfer from fibrinogen into film is discussed to directly correlate its anti-thrombogenicity.

## Materials and methods

### Synthesis of titanium oxide films

High purity (99.995%) titanium disk (12 mm diameter and 2 mm thickness) specimens were mechanically smoothed first by grinding with SiC paper progressively up to 4000 grits, and then polished with 0.5 µm diamond cloth. The specimens were cleaned in ultrasonic bath with acetone, ethanol and distilled water sequentially before deposition. The titanium oxide films were synthesized on the pure titanium matrix and silicon wafer by unbalanced magnetron sputtering (UBMS)

deposition, with titanium as metal arc source to produce metal plasma. The titanium plasma reacted with oxygen introduced (mixed with argon for enhanced excitation plasma) in the vacuum system, and the oxygen partial pressures were adjusted by flow ratio of oxygen/argon. The technique details of fabrication of the films are referred to Kelly and Arnell.[22] The Ti-O films with different stoichiometry of O/Ti ratio were obtained by controlling the flow of oxygen. The main instrumental conditions are shown in Table 1.

### Characterization

The chemical states of titanium, oxygen and carbon on near-surface (sputtered by around 5 nm) of the synthesized films were studied by X-ray photoelectron spectroscopy (XPS, Model PHI5600, Perkin-Elmer, USA) using monochromated Mg Ka X-rays operating at 14 kV. The spectra were curve-fitted using a computer-assisted Gaussian–Lorentzian peak model. The binding energy of the C 1s line was taken as $284.6 \pm 0.4$ eV for calibrating the obtained spectra. X-ray diffraction (XRD, X'Pert Pro MPD) were employed to characterize the structure of the films, with a glancing angle of 0.5° within a scanning range from 20° to 80°.

### Electrochemical impedance spectroscopy

Electrochemical impedance spectroscopy (EIS) offers a powerful method to analyze electrochemical behavior, in particular impedance feature of interfacial charge transfer between solid and solution. EIS measurements were conducted on an electrochemical workstation (IM6, Zahner, Germany), with a three-electrode setup electrochemical cell. A platinum slice was used as counter electrode, and a saturated calomel electrode (SCE) was employed as the reference electrode. The prepared Ti-O films samples deposited titanium (Ti-O/Ti) were taken as working electrode which were epoxy-resin-sealed to expose only researched Ti-O film surface. Phosphate buffered saline (PBS, pH 7.2, purchased from Sigma) and fibrinogen (human plasma fibrinogen purchased from Sigma-Aldrich)-containing PBS (PBS+Fbg, 2 mg/mL) were used as electrolytes. Spectra were obtained at open-circuit potential of the Ti-O/Ti sample in PBS and PBS + Fbg solution,

**Table 1.** Instrumental conditions of unbalanced magnetron sputtering preparation of Ti-O films.

| Samples | Bias voltage (V) | DC current (A) | Distance (mm) | Deposition time (min) | Ar/O ratio (SCCM) |
|---|---|---|---|---|---|
| Ti-O #1 | −150 | 3 | 80 | 20 | 60/14 |
| Ti-O #2 | | | | 10 | 60/9 |
| Ti-O #3 | | | | 8 | 60/7 |

with alternating applied potential of 5 mV amplitude, scanning from 10 kHz down to 1 mHz frequency. EIS spectra were recorded as Bode plot.

## Mott–Schottky plots

In principle, Mott–Schottky measurement is performed by capacitance and potential (C/E) testing, which is most suitable for semiconductor electrochemistry analysis. The Mott–Schottky was executed on the same electrochemical work station and arrangements for EIS, by scanning with DC potential (by potentiostate) from $-1.0$ V vs. SCE to 0.5 vs. SCE superimposed with an alternating potential of 5 mV at 1 kHz. Mott–Schottky plots were recorded directly, and analyzed by Mott–Schottky equation[23]

$$\frac{1}{C_{sc}^2} = \frac{2}{\varepsilon\varepsilon_0 e N_D}\left(E - E_{fb} - \frac{kT}{e}\right)$$

where $C_{sc}$ is the measured space-charge layer capacitance; $E_{fb}$ represents flat-band postential; $N_D$, the densities of donors in space-charge layer; $\varepsilon$, the relative dielectric coefficient of titanium oxide film. Space charge layer carrier concentration ($N_{SC}$ equivalent to donor density $N_D$) and $E_{fb}$ of the samples in PBS and PBS+Fbg were calculated by simulating the plot slope (using the above Mott–Schottky equation).

## Antithrombogenicity evaluation in vitro

The anti-thrombogenicity of the Ti-O films was evaluated in terms of in vitro blood compatibility/hemocompatibility testing, namely, fibrinogen activation, relative quantification of platelet adherent number, platelet adhesion morphology observation, as well as clotting time testing.

## Fibrinogen denaturalization

Fibrinogen denaturalization on material surface is an important stage of biomaterials-associated thrombosis, which can be detected by an indirect immunochemistry method with conformation-sensitive primary antibody.[15–17] Specifically, platelet-poor plasma (PPP, 50 μL) was added on each sample surface and incubated at 37°C for 2 h. Then the samples were blocked by bovine serum albumin (BSA) solution (1:100 diluted in PBS) for 30 min and then incubated with mouse anti-human fibrinogen γ chain antibody (Accurate, Westbury, NY, USA) (1/250 dilution in PBS) for 1 h. The samples were washed with PBS and incubated with horseradish peroxidase labelled goat anti-mouse antibody (Accurate, Westbury, NY, USA) (1/100 dilution in PBS) for another 1 h, washed and colored with tetramethylbenzidine

(TMB) chromogen. Absorbance was read at 450 nm on ELISA equipment by using microplate reader. The fibrinogen denaturalization was related to the absorbance and was calculated as percentage of activation by calibrating with absorbance data of blank PPP (i.e. over all fibrinogen in the 50 μL PPP as 100%), where $n = 6$ for all samples measurements.

## Lactate dehydrogenase activity measurement of platelet adherent numbers

The amount of adherent platelets on the sample surface was determined quantitatively by measuring the lactate dehydrogenase (LDH) activity, namely the occurrence of lysis on adhered platelets. The LDH samples measured 8 mm × 8 mm with 4 numbers in each group. Platelet-rich plasma (PRP, 50 μL) was dropped onto each sample in the assay kit, and then incubated at 37°C for 30 min. After rinsing with phosphate-buffered solution (PBS, 5 min × 3 times), Triton X-100 (diluted to 1%, 40 μL) was added onto the surfaces of the samples to lyse the adherent platelets for 5 min. Then lysates (25 μL) was taken from the surfaces and mixed with a substrate solution (β-Nicotinamide adenine dinucleotide, reduced disodium salt, trihydrate NADH, 200 μL) and sodium pyruvate in a 96-well plate. The concentration of adhered platelet on samples was colorimetrically measured as the optical density at 340 nm with a spectrometer (u-Quant, Bio-Tek Instruments Inc.). The nominal concentration represents the percentage of adhered platelet number in the total platelet number of 50 μL PRP.

## Platelet adhesion testing and morphology observation

PRP was prepared by centrifuging (1500 r/min, 15 min) fresh human whole blood. The samples of 8 mm × 8 mm size were ultrasonically cleaned by acetone, ethanol and distilled water and put in a silanized beaker. Then the samples were immersed in PRP (50 mL) and incubated at 37°C constant temperature for 30 min. After being washed with 0.9% NaCl solution, they were fixed using 2.5% glutaraldehyde solution for 12 h, then washed again with 0.9% NaCl three times, and subsequently immersed in 50%, 75%, 90% and 100% ethanol solutions for 10 min. After critical point drying (CPD030, ALZERS Company), samples were processed for observation by using field emission scanning electron microscopy (SEM, JSM-7001F, JEOL Ltd., Japan).

## Activated partial thromboplastin time and thrombin time

The activated partial thromboplastin time (aPTT) and thrombin time (TT) were measured on coagulometer

(ACL 200, Instrumentation Laboratory Co. USA). Fresh human PPP was prepared by centrifuging at 3000 r/min for 15 min. For the aPTT measurement, samples were attached to a 24-well culture plate. Fresh human PPP (200 μL) and actin-activated cephthaloplastin reagent (200 μL) were added, followed by the addition of 0.03 M $CaCl_2$ solution (200 μL) after incubation for 30 min at 37°C. The clotting time of the plasma solution was measured by using the coagulometer. In the case of the thrombin time (TT) measurements, 200 μL incubated PPP was dropped onto the surface of the samples. After incubation for 30 min at 37°C, the TT measurements were performed by adding 200 μL incubated PPP solution into 200 μL TT reagent in a test tube, and then was measured by using the same coagulometer.
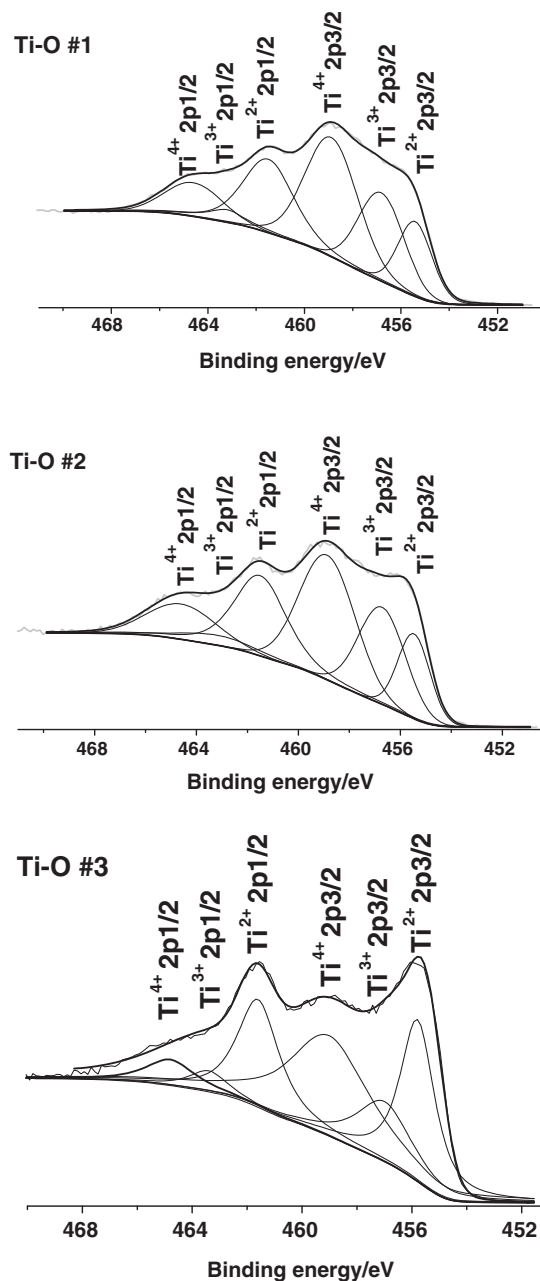
## Results

### XPS spectra and XRD pattern

Surface chemical state of the prepared Ti-O films was revealed by Ti 2p XPS core level spectra as depicted in Figure 1. The two overlapped band of Ti 2p1/2 and Ti 2p3/2 can be de-convoluted as $Ti^{2+}$, $Ti^{3+}$ and $Ti^{4+}$ bonding states respectively, through curve-fitting by Gaussian–Lorentzian peak model.[24] The fitting results of crystalline atom O/Ti ratio by Ti 2p XPS core level spectra of the prepared Ti-O films are shown in Table 2. Accordingly, with the decrease of oxygen partial pressure during deposition, the Ti-O films were obtained with reduced percentage of $Ti^{4+}$ and relatively higher percentage of $Ti^{3+}$ and $Ti^{2+}$. The crystalline O/Ti ratio of sample Ti-O #1, Ti-O #2 and Ti-O #3 decreased from 1.56 to 1.49 and 1.43, suggesting that the Ti-O films are all sub-stoichiometric titanium oxides.

Crystalline structure of the films is described by the XRD patterns and identified as shown in Figure 2.[25] Ti-O #1 sample was identified as mostly mixture existence of rutile (R) $TiO_2$ and anatase (A) $TiO_2$ phase structure. Ti-O #2 showed two $Ti_2O_3$ peaks, mixed mainly with R&A$TiO_2$ peaks. Ti-O #3 sample appeared to consist of more $Ti_2O_3$ and TiO phases. The change of X-ray diffraction patterns of the prepared Ti-O samples with decreasing of oxygen partial pressure indicates that the structure of Ti-O films changed gradually from mostly rutile and anatase $TiO_2$ to $Ti_2O_3$ and TiO with lower degree of crystallinity.

### EIS spectra

Interfacial electrochemical behavior of titanium oxide films in contact with fibrinogen containing phosphate buffer saline can be well disclosed by their electrochemical impedance spectra to reveal all the invloved



**Figure 1.** Ti 2p X-ray photoelectron spectra of the prepared Ti-O films (10 nm sputtering depth).

**Table 2.** The fitting results of crystalline O/Ti ratio by Ti 2p X-ray photoelectron spectroscopy core level spectra and Ti atom valence percentage of the prepared Ti-O films.

| Samples | O/Ti ratio | Valence percentage of Ti atom (%) | | |
|---------|-----------|-----------|-----------|-----------|
| | | $Ti^{2+}$ | $Ti^{3+}$ | $Ti^{4+}$ |
| Ti-O #1 | 1.56 | 31.1 | 26.3 | 42.6 |
| Ti-O #2 | 1.49 | 35.4 | 31.0 | 33.6 |
| Ti-O #3 | 1.43 | 42.5 | 29.0 | 28.5 |
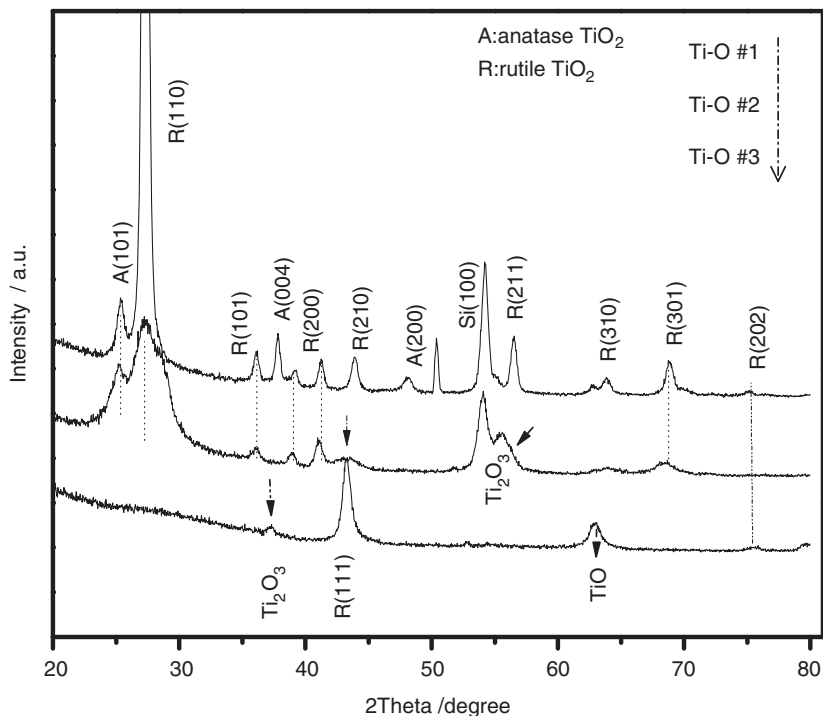
**Figure 2.** X-ray diffraction patterns of Ti-O films.

reactions, particularly including interfacial charge transfer reaction resistance. Figure 3 shows EIS bode spectra of the prepared Ti-O films in PBS and PBS + Fbg. Both in PBS and PBS + Fbg, at highest frequency of $10^5$ Hz, impedance was attributed by solution resistance solely. At frequency range of 1000 to 1 Hz all Ti-O films appeared to have an increasing linear impedance plot with decreasing of frequency. The acompanying phase angles showed that there were two time constant element (CE), which were overlapped over the range. The first phase peak at around $1.05 \times 10^2$ Hz is contributed to space charge layer capacitance $C_{sc}$ and resistance of Ti-O film $R_f$; the second at around $9.8 \times 10^{-1}$ Hz is contributed to double layer capacitance $C_{dl}$ and interfacial reaction resistance $R_{ct}$ (as the indicator of the degree of difficulty for charge transfer from solution into Ti-O films). At $10^{-3}$ Hz, the impedance reached the highest and tend to be more slightly increased, which is ascribed to the Wargburg element of diffusion-controlled process. In PBS, the Ti-O #1 seemed to have the highest interfacial reaction resistance $R_{ct}$, and Ti-O #2 and Ti-O #3 had similarly lower $R_{ct}$. Whereas in PBS + Fbg, both Ti-O #1 and Ti-O #3 showed obvious decreased $R_{ct}$, Ti-O #2 showed ingnorable change (slighly increased) of $R_{ct}$ when in contact with fibrinogen containing PBS as compared to pure PBS. This revealed that Ti-O #2 has the highest interfacial reaction resistance to prevent fibrinogen charge tranfer onto film surface.

## Mott–Schottky plots

One of the important features of semiconductor electrochemistry is the space charge layer built up on semiconductor surface when in contact with electrolyte, owing to their separeted energy level and tendancy to reach an equilibrium of accumulation of charge at the interface. Mott–Schottky relation exists at the interface and is employed to dictate the electronic structure (positon of the energy band) of interface as well as doping states (carriers density).[23] Figure 4 depicts experimental measure and linear fit of Mott–Schottky plots of Ti-O samples in both PBS and PBS + Fbg. All the plots presented a positive slope around rest-open potential of the samples, indicating that all the Ti-O films are n-type semiconductor. Space charge layer carrier concentration $N_{sc}$ and flat energy band potential $E_{fb}$ of the three Ti-O films samples in PBS and PBS + Fbg were calculated and are listed in Table 3. Ti-O #1 possessed apparently low $N_{sc}$ and relatvely positive $E_{fb}$, indicating low degree of n-type doping. In contrast, Ti-O #2 and Ti-O #3 both produced significantly higher (about over 2 orders) $N_{sc}$ value as well as more negative $E_{fb}$ compared to Ti-O #1, indicating that they were highly doped. Note Ti-O film 2# presented the most negative flat energy band potential and highest carrier concentration even when in contact with Fbg containing PBS, while Ti-O #3 showing an extra linear section at more anodic scanned range can
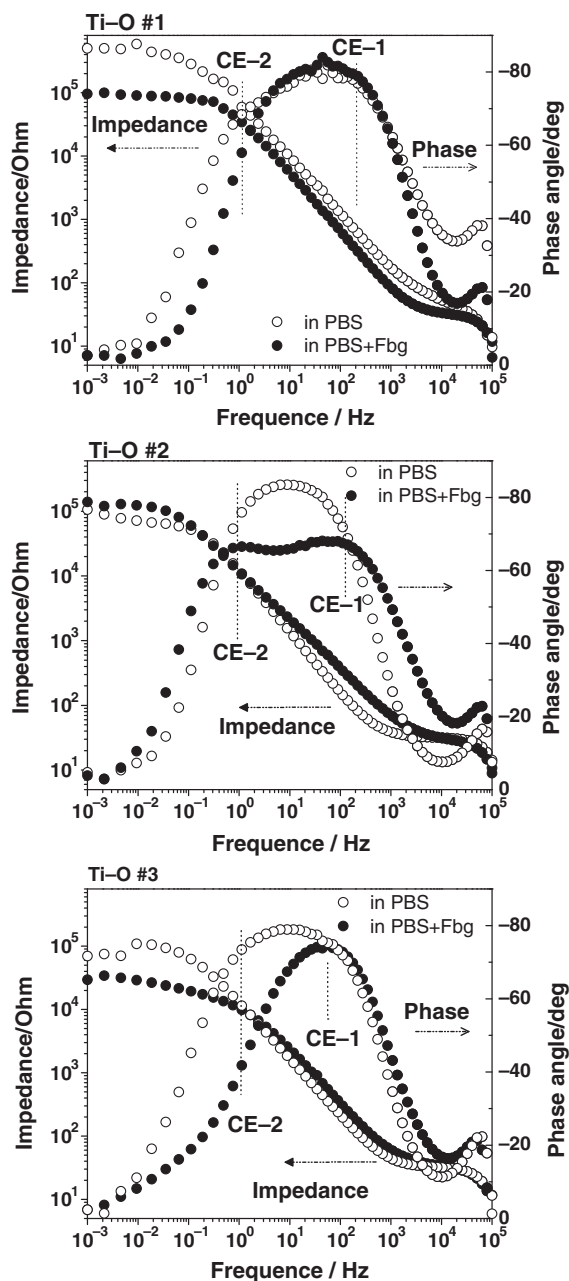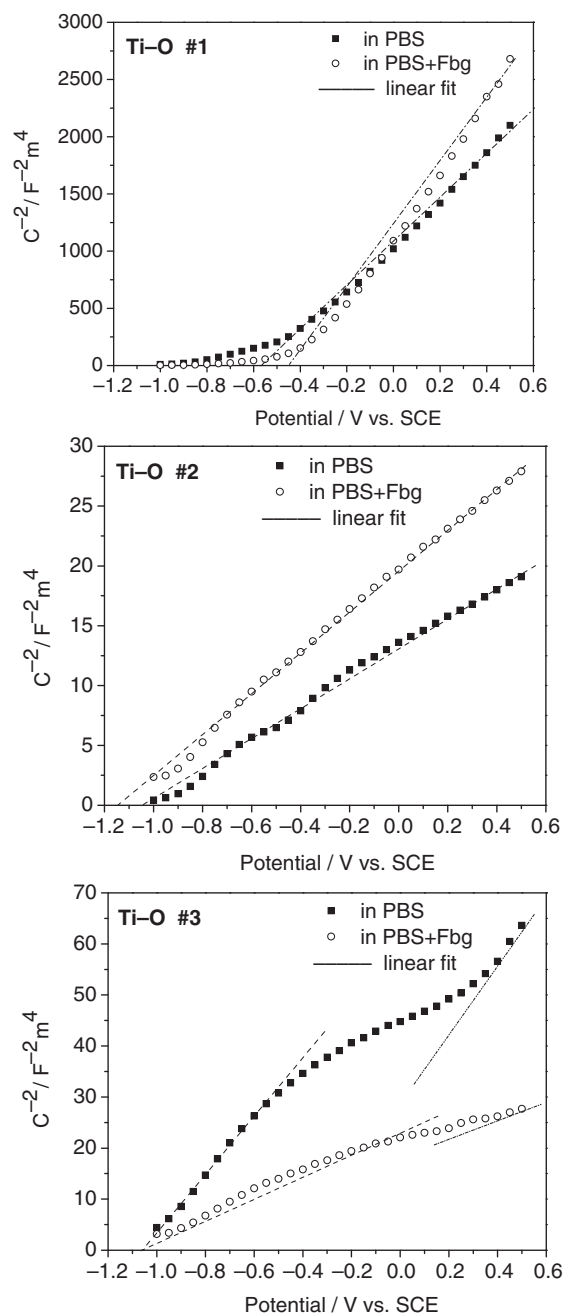
**Figure 3.** Electrochemical impedance spectroscopy Bode spectra of Ti-O samples in PBS and PBS + Fbg (2 mg/mL) solutions.
PBS: phosphate buffered saline.



**Figure 4.** Experimental measure and linear fit of Mott–Schottky plots of Ti-O samples in PBS and PBS + Fbg (2 mg/mL) solutions.
PBS: phosphate buffered saline.

be assigned to TiO phase contribution other than TiO$_2$ phase.

### Fibrinogen denaturalization

The interfacial charge transfer facilitates conformational change and hence chemical activation of fibrinogen,[20,26] which can be illustrated by fibrinogen denaturalization results as plotted in Figure 5. Ti-O #2

film showed significantly least degree of Fbg activation, whereas both Ti-O #1 and Ti-O #3 produced severe degree of Fbg denaturalization, and the Ti-O #1 looked severest.
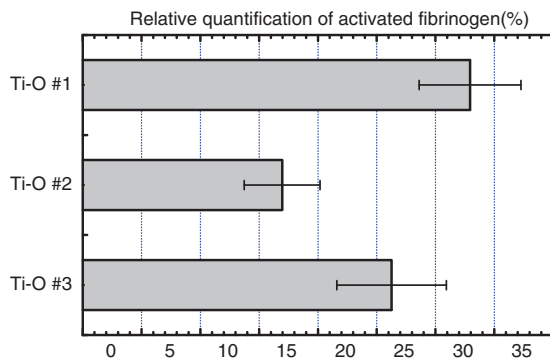
### Lactate dehydrogenase assay

Higher levels of the surface adsorption and activation of fibrinogen correlates with the adhesion and

**Table 3.** Calculated carrier concentration $N_{sc}$ and flat energy band potential $E_{fb}$ of the films.

| Sample | $E_{fb}$ (V vs. SCE) | | $N_{sc}$ (cm$^{-3}$) | |
|---|---|---|---|---|
| | In PBS | In PBS + Fbg | In PBS | In PBS + Fbg |
| Ti-O #1 | −0.62 | −0.44 | 3.7E18 | 3.3E18 |
| Ti-O #2 | −1.05 | −1.16 | 7.4E20 | 5.6E20 |
| Ti-O #3 | −1.04 | −1.08 | 1.6E20 | 4.1E20 |

PBS: phosphate buffered saline.



**Figure 6.** Lactate dehydrogenase testing results of the platelets adherent number on the prepared Ti-O films ($n = 6$) with platelet-rich plasma.
***$p < 0.001$ compared to platelets number in 50 μL platelet-rich plasma as reference; **$p < 0.005$ compared to platelets number in 50 μL platelet-rich plasma reference.



**Figure 5.** Fibrinogen denaturalization results of the prepared Ti-O films surface ($n = 6$).
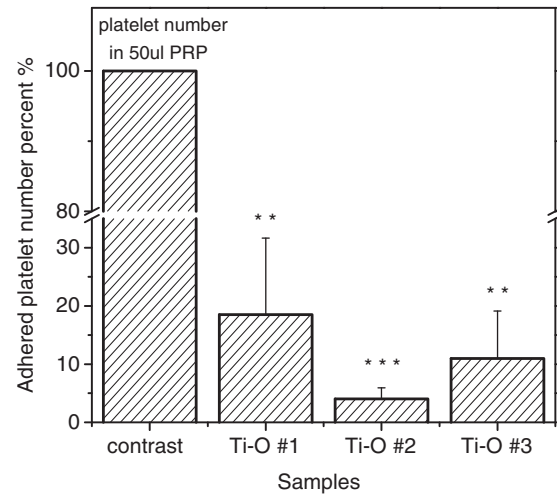
aggregation of platelets on biomaterial surfaces.[27] According to LDH results as shown in Figure 6, the adhered platelet number on the Ti-O #2 sample are significantly lower than Ti-O #1 and Ti-O #3, which is consistent with Fbg denaturalization results.

## Morphology observation of platelets adhesion testing

Morphology of platelet has been well-established as a dictator of the extent of activation of platelets on foreign surfaces.[28] Morphologies of adherent platelets on Ti-O films by SEM observation are displayed in Figure 7. Ti-O #2 appeared as natural round states with less deformation; whereas serious pseudopodium and aggregation occurred on Ti-O #3 and most severely spreading activation were observed on Ti-O #1 surface.

## Activated partial thromboplastin time and thrombin time

Activated partial thromboplastin time (aPTT) provides a simple and reliable measurement of the capacity of blood to coagulate through intrinsic coagulation mechanism involving the effect of the biomaterial on delay of the process. The activation on material surface takes place via combined interactions among the coagulation factors, for example, factor X activates and transforms

into factor Xa, factor Xa activates prothrombin (factor II) to thrombin (factor IIa), and thrombin prompts fibrinogen transform to fibrin, then the cascade of coagulation proceeds until blood is clotted.[29] The TT test is used to evaluate the interval of activation of fibrinogen to fibrin. All the three Ti-O films prolonged aPTT and TT time (Figure 8) as compared to the orinal plasma, among them Ti-O #2 film showed significantly higher value. The delayed clotting time results were consistent with fibrinogen activation and platelets adhesion results.
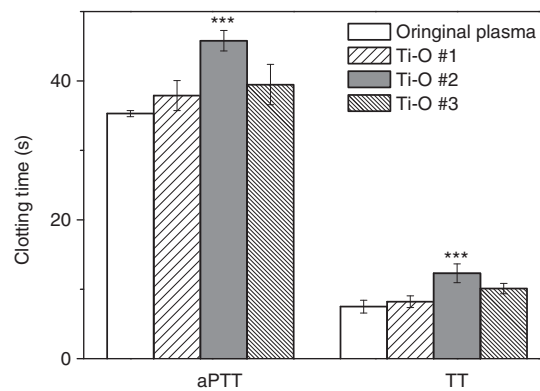
## Discussion

The first major phenomenon when biomaterial is in contact with blood is adsorption of plasma proteins such as fibrinogen and albumin. The proteins involved in coagulation might undergo conformational change and further chemical activation.[26] Then, platelet cells are likely to interact with these proteins and the solid surface to produce adhesion, aggregation and activation, finally triggering cascade reactions of thrombosis.[27,30] Such process of thrombosis on material surface is considered via silmilar pathology intrinsic pathway of coagulation, involving a number of coagulation factors with complicated interactions.[2,3] It has been shown that biomaterial-associated thrombosis is accompanied with charge (electrons) transfer from the inactive state of fibrinogen to the surface of the biomaterial,[15–17] which causes fibrinogen to decompose into monomers and peptides (denaturalization and activation). The resulting monomers then polymerize into
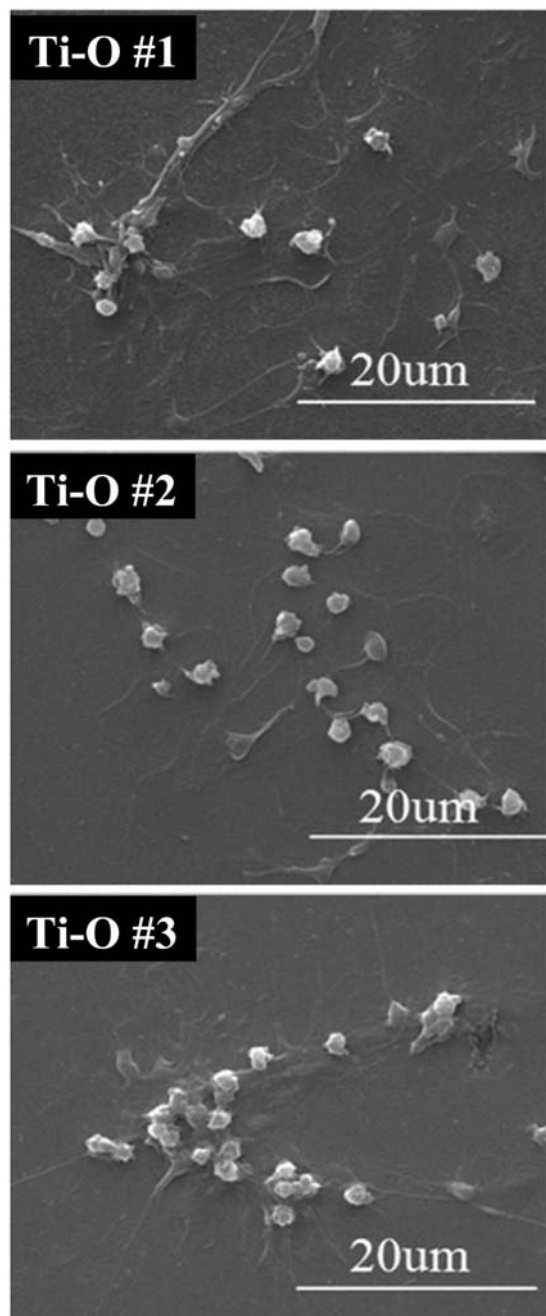
**Figure 7.** Representative scanning electron microscopic photos of adherent platelet morphology on Ti-O films with platelet-rich plasma for 30 min.



**Figure 8.** Activated partial thromboplastin time (aPTT) and thrombin time (TT) results of Ti-O films ($n = 6$) with platelet-poor plasma.
***$p < 0.005$ compared to original plasma as reference.

insoluble fibrin, and the cross-linked fibrins meshed with platelets and red cells finally lead to an irreversible thrombus. According to the electrochemical mechanism, intuitively, the biomaterials that will inhibit charge transfer from fibrinogen onto its surface could perform good anti-thrombogenicity. This has been proven reportedly on metals, i.e. active metals with more cathodic electromotive force, like magnesium, are more anti-thrombogenic due to higher Fermi levels as compared to noble metals in the anodic side of electromotive series.[31] Nevertheless, based on metal electrochemistry theory, both cathodic and anodic direction of charge transfer at the metal/electrolyte interface are always inevitable as the metals' Fermi levels are readily adjusted to electrochemical energy level of solution (electrolyte), i.e. fibrinogen activation always occurs inevitably in such case. This might be the reason why metals possess unsatisfying anti-thrombgenicity.[31,32]

In contrast to metals, semiconductor electrode provides independent surface energy level (for example, the bottom of conduction band $E_{sc}$ and the top of valence band $E_{sv}$) with regard to electrochemical energy level of electrolyte (fibrinogen herein).[23,33] As illustrated in Figure 9, according to semiconductor electrochemistry,[33] the difference in energy level on two sides of solid/solution interface is actually fixed, and determines the charge transfer direction thermodynamically and the reaction resistance kinetically. For n-type widegap semiconductor titanium oxide (3.0–3.2 eV), the high level of doping gives rise to higher carrier density (or electrons donor) in space charge layer, which prevent electron transfer from fibrinogen; in addition, more negative flat-band potential relates to higher position at the bottom of conduction band $E_{sc}$ energy level, then higher energy barrier $\Delta\Phi$ is thus built up between fibrinogen and semiconductor, therefore giving rise to larger resistance to charge transfer from fibrinogen to Ti-O films.

Our prepared Ti-O films are all substoichiometric, and the O deficiency are likely to produce Ti 3d orbital energy levels n-type doping, similar to oxygen vacancy n-doping mechanism in $TiO_2$.[25] Ti-O #1 consists of more stoichiometric $TiO_2$ crystalline phase, and provide apparently low carrier concentration in space charge layer as well as relatively more postive flat-band potential (lower position of conduction
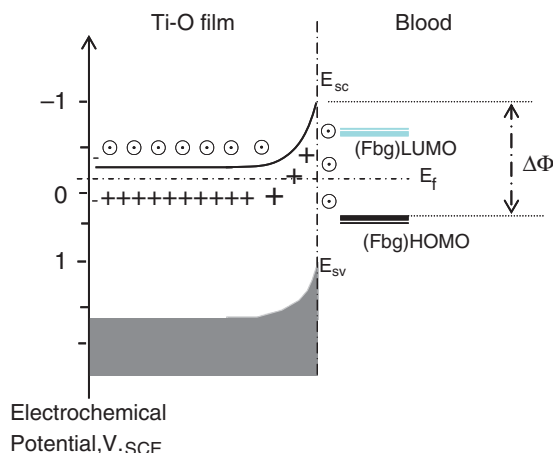
**Figure 9.** Schematic of electronic structure and energetic of Ti-O film/blood (fibrinogen) interface.

band bottom). Ti-O #2 and Ti-O #3 have obviously higher degree of doping with lower O/Ti ratio, leading to increased surface carrier concentration and higher Fermi levels,[33] and the electrons tend to escape from the Ti-O film, i.e. the charge transfer from fibrinogen to Ti-O film is inhibited more efficiently. Nevertheless, Ti-O #3 possess more $Ti_2O_3$ and particularly TiO phase which provide a lower degree of doping in whole film as well as an extra lower conduction band position beyond that of $TiO_2$ phase,[34] which can be ascertained by Mott–Shottky plot, where there appears an extra linear section at more anodic scanning range. This could reduce the energy position barrier and probably allow more charge transfer from fibrinogen to Ti-O films.[35] In short, the anti-thrombogenicity of titanium oxide films seems dependent upon the unique semiconducting property. The n-type characteristic with space charge layer of high density donor states and higher position of surface energy level ($E_{sc}$) plays a decisive role in establishment of an electrochemical interfacial energy barrier. Such barrier will largely reduce the risk of fibrinogen activation by preventing its electrons charge transfer toward Ti-O films, which subsequently results in less possibility of platelets activation and finally good anti-thrombogenicity.[35]

The electrochemical behavior of the real semiconductor–blood interface might not only be used to better understand the biomaterials-associated thrombosis,[36,37] but possibly also provide an important criterion to screen or optimize anti-thrombogenic semiconducting biomaterials like Ti-O films and others.[38–40]

## Conclusion

In this article, we prepared sub-stoichiometric Ti-O films of three O/Ti ratios. All the Ti-O films are

n-type semiconductor, but offered different degrees of doping as well as surface energy level position. We found that the anti-thrombogenicity of Ti-O films correlated directly with their interfacial electrochemical behaviors in fibrinogen containing phosphate buffer solution, and is sensitively related to their stoichiometric O/Ti ratio and crystalline phase structure. A rationale of energetics of the semiconductor Ti-O film/fibrinogen interface was discussed, and is proposed to guide further improvement in antithrombogenicity of semiconducting biomaterials. A sufficient energy barrier between the fibrinogen in blood and the biomaterials will be needed to inhibit fibrinogen activation by preventing charge transfer onto the biomaterials surface, eventually lessening the likelihood of triggering the cascade blood coagulation reactions, and therefore finally avoiding thrombosis. More specifically for titanium oxide films, those with higher degree of inherent n-type doping would best prevent the charge transfer from fibrinogen (namely its activation), and hence potentially serve best for surface-modification of blood-contacting implantable devices such as cardiovascular stents and artificial heart valves. The future work might focus more on effective ways to impede the charge transfer, as well as taking systematic considerations thereof in the whole picture of real interfacial electrochemical interactions between blood and the semiconducting biomaterials.

## References

1. Williams DF. On the mechanisms of biocompatibility. *Biomaterials* 2008; 29: 2941–2953.
2. Ratner BD. The catastrophe revisited: blood compatibility in the 21st century. *Biomaterials* 2007; 28: 5144–5147.
3. Gorbet MB and Sefton MV. Biomaterial-associated thrombosis: roles of coagulation factors, complement, platelets and leukocytes. *Biomaterials* 2004; 25: 5681–5703.
4. Vogler EA and Sledlecki CA. Contact activation of blood-plasma coagulation. *Biomaterials* 2009; 30: 1857–1869.
5. O'Brien B and Carroll W. The evolution of cardiovascular stent materials and surfaces in response to clinical drivers: a review. *Acta Biomater* 2009; 5: 945–958.
6. Bakir M. Haemocompatibility of titanium and its alloys. *J Biomater Appl* 2012; 27: 3–15.

7. Huang N, Yang P, Leng YX, et al. Hemocompatibility of titaniumoxide films. *Biomaterials* 2003; 24: 2177–2187.

8. Huang N, Yang P, Cheng X, et al. Blood compatibility of amorphous titanium oxide films. *Biomaterials* 1998; 19: 771–776.

9. Maitz MF, Pham MT, Wieser E, et al. Blood compatibility of titanium oxide with various crystal structure and element doping. *J Biomater Appl* 2003; 17: 303–319.

10. Liu XH, Zheng ZH, Zhou ZY, et al. Surface modification of titanium based biomaterials by ion beam. *J Biomater Appl* 1996; 10: 330–337.

11. Zhang F, Liu XH, Mao YJ, et al. Artificial heart valves: improved hemocompatibility by titanium oxide coatings prepared by ion beam assisted deposition. *Surf Coat Technol* 1998; 103-104: 146–150.

12. Liu JX, Yang DZ, Shi F, et al. Sol–gel deposited TiO$_2$ film on NiTi surgical alloy for biocompatibility improvement. *Thin Solid Films* 2003; 429: 225–230.

13. Chu CL, Wang RM, Hu T, et al. XPS and biocompatibility studies of titania film on anodized NiTi shape memory alloy. *J Mater Sci Mater Med* 2009; 20: 223–228.

14. Wang XH, Yu LJ, Li CR, et al. Competitive adsorption behavior of human serum albumin and fibrinogen on titanium oxide films coated on LTI-carbon by IBED. *Colloid Surf B: Biointerfaces* 2003; 30: 111–121.

15. Sawyer PN. Significance of electrochemical phenomena in intravascular thrombosis. *Nature* 1965; 206: 1162–1163.

16. Sawyer PN, Srinivasan S, Chopra PS, et al. Electrochemistry of thrombosis - an aid in the selection of prosthetic materials. *J Biomed Mater Res* 1970; 4: 43–55.

17. Baurschmidt P and Schaldac M. The electrochemical aspects of the thrombogenicity of a material. *J Bioeng* 1977; 1: 261–278.

18. Bolz A, Amon M, Ozbek C, et al. Coating of cardiovascular stents with a semiconductor to improve their hemocompatibility. *Tex Heart Inst J* 1996; 23: 162–166.

19. Shih CC, Shih CM, Su YY, et al. The interaction of selected semiconducting biomaterials with platelet-rich plasma and whole blood. *J Biomed Mater Res Part A* 2005; 74A: 325–337.

20. Gettens RTT and Gilbert JL. Fibrinogen adsorption onto 316 L stainless steel under polarized conditions. *J Biomed Mater Res Part A* 2008; 85: 176–187.

21. Shih CC, Shih CM, Su YY, et al. Quantitative evaluation of thrombosis by electrochemical methodology. *Thromb Res* 2003; 111: 103–109.

22. Kelly PJ and Arnell RD. Magnetron sputtering: a review of recent developments and applications. *Vacuum* 2000; 56: 159–172.

23. Bott AW. Electrochemistry of semiconductors. *Curr Separat* 1998; 17: 87–91.

24. Wanger CD, Riggs WM, Davis LE, et al. *Handbook of X-ray photoelectron spectroscopy*, 1st ed. Eden Prairie, MN: Perkin–Elmer, pp.68–70.

25. Diebold U. Structure and properties of TiO2 surfaces: a brief review. *Appl Phys A* 2003; 76: 681–687.

26. Clarke ML, Wang J and Chen Z. Conformational changes of fibrinogen after adsorption. *J Phys Chem B* 2005; 109: 22027–22035.

27. Gibbins JM. Platelet adhesion signaling and the regulation of thrombus formation. *J Cell Sci* 2004; 117: 3415–3425.

28. Packham MA. The behaviour of platelets at foreign surfaces. *Proc Soc Exp Biol Med* 1988; 189: 261–274.

29. Vroman L. What factors determine thrombogenicity. *Bull N Y Acad Med* 1972; 48: 302–310.

30. Guha Thakurta S, Miller R and Subramanian A. Investigation of platelet responses and clotting characteristics of in situ albumin binding surfaces. *J Biomater Appl* 2012; 26: 529–547.

31. Sawyer PN and Srinivasan S. Relation between thrombosis on metal electrodes and the position of metal in the electromotive series. *Nature* 1967; 215: 1494.

32. Hong J, Azens A, Ekdahl KN, et al. Material-specific thrombin generation following contact between metal surfaces and whole blood. *Biomaterials* 2005; 26: 1397–1403.

33. Morrison SR. *Electrochemistry at semiconductor and oxidized metal electrodes*, 1st ed. New York: Plenum Press, pp.59–75.

34. Botha SJ. Surface properties and bio-acceptability of Ti2O3 surfaces. *Mater Sci Eng A* 1998; 243: 221–230.

35. Shih CC, Shih CM, Su YY, et al. Characterization of the thrombogenic potential of surface oxides on stainless steel for implant purposes. *Appl Surf Sci* 2003; 219: 347–362.

36. Mani G, Feldman MD, Patel D, et al. Coronary stents: a materials perspective. *Biomaterials* 2007; 28: 1689–1710.

37. Hu WJ, Eaton JW, Ugarova TP, et al. Molecular basis of biomaterial-mediated foreign body reactions. *Blood* 2001; 98: 1231–1238.

38. Jayabalan M. Biological interactions: causes for risks and failures of biomaterials and devices. *J Biomater Appl* 1993; 8: 64–71.

39. Courtney JM, Lamba NMK, Sundaram S, et al. Biomaterials for blood-contacting applications. *Biomaterials* 1994; 15: 737–744.

40. Ratner BD, Hoffman AS, Schoen FJ, et al. *Biomaterials science: an introduction to materials in medicine*, 2nd ed. San Diego: Academic Press, pp.367–378.